





Research Article

Design and Control of Modified Resonant Voltage Multiplier Rectifier for Photovoltaic Applications Using Electrolytic Capacitive Material

Sathish Kumar Shanmugam ¹, **C. Subba Rami Reddy**,² **S. V. G. V. A. PRASAD**,³
Bharath Kumar Narukullapati ⁴, **R. Ramkumar**,⁵ **G. G. RajaSekhar**,⁶ **G. Subramaniam** ⁷,
M. Sivachitra ⁸, **L. Anbarasu**,⁹ and **Nyagong Santino David Ladu** ¹⁰

¹Department of Electrical and Electronics Engineering, M.Kumarasamy College of Engineering, Karur, Tamil Nadu, India

²Department of Electrical and Electronics Engineering, B V Raju Institute of Technology, Vishnupur, Narsapur, Medak, Telangana, India

³Department of Physics, Pithapur Rajah's Government Autonomous College, Kakinada, Andhra Pradesh, India

⁴Department of Electrical and Electronics Engineering, Vignan's Foundation for Science Technology and Research Vadlamudi, Guntur, Andhra Pradesh, India

⁵Department of Electrical and Electronics Engineering, Dhanalakshmi Srinivasan University, Trichy, Tamil Nadu, India

⁶Department of Electrical and Electronics Engineering, Koneru Lakshmaiah Education Foundation, Guntur, Andhra Pradesh, India

⁷Department of Electrical and Electronics Engineering, M.Kumarasamy College of Engineering, Karur, Tamilnadu, India

⁸Department of Electrical and Electronics Engineering, Kongu Engineering College, Perundurai, Tamilnadu, India

⁹Department of Electrical and Electronics Engineering, Erode Sengunthar Engineering College, Perundurai, Tamilnadu, India

¹⁰Department of Mathematics and Physics, Rumbek University of Science and Technology, South Sudan

Correspondence should be addressed to Sathish Kumar Shanmugam; sathishphd2k17@gmail.com and Nyagong Santino David Ladu; nyagongsantino19@gmail.com

Received 11 May 2022; Revised 28 May 2022; Accepted 2 June 2022; Published 7 July 2022

Academic Editor: Samson Jerold Samuel Chelladurai

Copyright © 2022 Sathish Kumar Shanmugam et al. This is an open access article distributed under the Creative Commons Attribution License, which permits unrestricted use, distribution, and reproduction in any medium, provided the original work is properly cited.

In this paper, a modified resonant voltage multiplier rectifier (RVMR) has been developed to improve the voltage gain and efficiency of the proposed converter on PV interconnected renewable energy systems. To acquire the most energy from the PV source, the improved RVMR scheme uses an altered Perturb and Observe (P&O)-based MPPT approach. This paper develops a modified variable step size P&O MPPT algorithm that can increase the PV system's dynamic and steady-state performance at the same time. The recommended variable step size technique addresses the constraints of traditional P&O MPPT. The suggested study uses the MATLAB/Simulink environment to analyze and evaluate voltage gain and efficiency.

1. Introduction

PV systems typically produce a low DC output voltage. When the panels are connected in a cascade, a larger DC voltage is generated. However, the cascading of panels causes a voltage imbalance at the module level. Because power generation fluctuates with sun irradiation, it is necessary to get the highest power output from the solar panel. As a

result, by using high gain converters, the technique to cascading the panels for higher voltage generation can be enhanced. The converters used for high gain conversion should have a high voltage gain ratio and be efficient. Static gain is high. Due to the growing demand for applications when combined with low voltage sources such as renewable energy sources and battery-powered systems, DC-DC converters are currently a major research focus [1–5]. The suggested work

employs a static high gain, high efficiency DC-DC converter to produce a greater static gain and more efficient power conversion. When integrating low voltage input sources with the grid, this helps to get the intended output. The boost converter is a type of DC-DC converter that is not isolated. With an output voltage of roughly five times the input voltage and a duty cycle (D) of 0.8, it can generally run with appropriate static and dynamic performance. Classic boost converters require huge switch duty ratios to generate substantial voltage increases. Excessive current stress in the boost switch is caused by high duty cycles. The parasitic resistive components in the circuit limit the greatest voltage gain that can be attained, and the efficiency is severely lowered for higher duty ratios. Because the diode only conducts for a brief time, there are issues with reverse recovery. [1–3, 6–10].

The Vienna rectifier was first introduced in 1997 and was utilized in communication power supply systems. Due to its multiple advantages over other known topologies, this rectifier is an excellent choice for use in a WECS. Its input power factor is closer to unity, and it has low harmonic distortion input currents. This three-level converter contains only three controlled switches that are subjected to minimal voltage stress, resulting in lower costs and easier switching control. Another benefit of this rectifier is its high efficiency. This converter has no dead time. It can work at high frequencies, and the currents do not have any dead time harmonics. Because the Vienna rectifier is a unidirectional converter, its use in other industries, such as electric train systems, has been limited. Active power flows only from the generator side to the load in WECSs. As a result, the Vienna rectifier is an excellent choice [4].

2. Modified Isolated Resonant Converter with a Resonant Voltage Multiplier Rectifier (RVMR)

Because of their galvanic isolation capabilities on both the source and load sides, isolated high step-up converters are favored. Because the efficiency of isolated converters is highly dependent on it, they prefer transformer-based isolation. The isolation part is impossible to detect without transformers. The greatest power can be delivered, however, if the transformer is operated at its maximum resonant state. As a result, in that situation, a resonant converter would be the better option. This paper proposes a resonant converter-based step-up configuration with good gain and efficiency.

A nearly sinusoidal current occurs at the resonant input, allowing switching devices to perform zero voltage switching (ZVS) or zero current switching (ZCS). As a result, switching losses can be greatly decreased, and far higher switching frequencies can be achieved [11, 12]. This indicates that the resonant converters are being used effectively for high step-up conversions. The purpose of this project is to illustrate design issues for an isolated high step-up converter based on a full-bridge topology with integrated voltage addition, which reduces voltage stress on the converter switches. [4]

For a low voltage input renewable system, an isolated high step-up step-down converter has been built to bring

the low voltage source to meet the grid requirements. Soft-switching techniques are used to reduce switching losses and increase the efficiency of the converter. This paper proposes a modified isolated resonant converter featuring a RVMR, primary-side fixed frequency switching, and secondary-side phase-shift control [2, 5, 13–19].

2.1. Resonant Voltage Multiplier Rectifier. The principal side circuit is chosen according to the needs of practical applications and is not restricted to those indicated in Figure 1. RCs are obtained by combining a correct primary-side circuit with the planned RVMR [7]. An example configuration with a full-bridge input stage and an N-type RVMR is shown in Figure 1.

3. Modified Resonant Voltage Multiplier Implementation for PV Integration

To investigate the key parameter design issues, a 50 V-70 V input and 415 V/425 W output model operating at a 100.1 kHz switching frequency was used as an example. The two primary constraints when determining the characteristics of a resonant tank, L_r and C_r , are the resonant frequency and output power.

The equation depicts the relationship between resonant capacitance voltage ripple and output power (1). The maximum voltage ripple should be less than half of the output voltage, which is the DC voltage of the capacitor. As a result, the resonant capacitance value should fulfill

$$C_r > \frac{P_o T_s}{2V_o^2}. \quad (1)$$

$C_r > 13.5 \text{ nF}$ is produced by replacing $V_o = 415 \text{ V}$, $P_o = 425 \text{ W}$, and $T_s = 10.12 \text{ s}$. Equation (2) should be satisfied by the resonant inductor L_r .

$$L_r < \frac{V_o^2}{2\omega^2 P_o T_s}. \quad (2)$$

$L_r 101.2 \text{ H}$ is produced by inserting the parameters into Equation (5.3). Because the voltage stresses on these devices are $0.51V_o + V_{Cr}$, having a larger C_r and a smaller L_r lowers the peak voltage on C_r , which is preferable for lowering the peak voltage on secondary-side active switches S5 and S6 and diodes D1 and D4.

However, a higher C_r value will increase the resonant capacitance's size and volume. 22.23 nF two capacitors are employed as resonant capacitors, taking into mind the value of the actual capacitors. The peak voltages of S5 and S6 and D1 and D4 are roughly 415 V and 419 V, respectively, according to Equation (1), so devices with the appropriate rating can be utilized.

Figure 2 shows that the block diagram of modified resonant voltage multiplier rectifier.

3.1. Modified Perturb and Observe (P&O) MPPT Algorithm for Proposed Topology. Photovoltaic (PV) arrays turn sunlight into electricity in general. The amount of DC power generated is determined by solar illumination and ambient

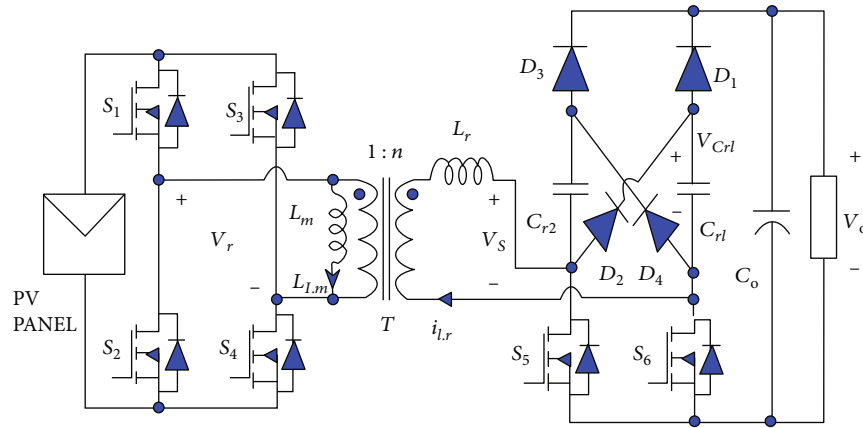


FIGURE 1: N type RVMR full-bridge resonant converter.

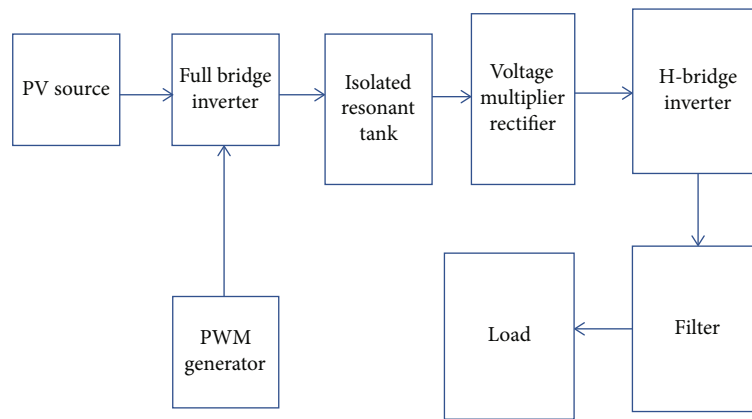


FIGURE 2: Modified resonant voltage multiplier rectifier block diagram.

temperature. It also fluctuates depending on the weight of the load. Under uniform irradiance and temperature, a PV array has a current-voltage characteristic with a single point, dubbed the maximum power point, where the PV array produces its maximum output power.

The maximum power point tracking (MPPT) technique is required for PV arrays to give maximum power to loads. In a nutshell, the MPPT algorithm continuously detects the PV array's instantaneous maximum power [5, 16–18].

Incremental conductance, fractional, fuzzy logic or neural network, open-circuit voltage current sweep, DC-line capacitor droop control, load current or voltage control, ripple correlation control, and dP/dV or dP/dI feedback control are just a few of the MPPT methods that have recently been developed and implemented. Convergence speed is one of the parameters used to evaluate and compare MPPT algorithms, especially during crucial weather change conditions. Many studies have been conducted to address this problem, but the accuracy and search time are constantly being improved. [2, 3]

The modified Perturb and Observe (P&O)-based maximum power point tracking technique was utilized to extract the maximum power from the PV input source in order to accomplish rapid and reliable maximum power point opti-

mization. Because PV panels are exposed to environmental changes, a maximum power tracking technique is required to harvest the maximum power from them. The duty ratio of the converter is changed as the PV panels are connected to the front side of the complete bridge controller to maintain maximum power tracing. The duty ratios of the complete bridge converters, which are triggered with an alternate duty control, are changed to extract the maximum power from the PV panels [2, 5, 6, 19].

The power is extracted using the modified P&O technique. The voltage input, as well as the sun irradiance and current, are required by the P&O controller. The converter is used to determine the power change by comparing the input and output power. The approach distinguishes between cyclic power variations and changes in power fluctuations. The P&O controller compares the changes in voltage and power and then determines the perturbation direction. The power is used to calculate the duty cycle. The duty ratio is regulated while the PV panel is operating in the MPP region. When PV panels are placed in non-MPP zones, however, the step size discrepancies are much bigger. Thus, under any scenario, the controller adjusts the PV panel to trace its maximum power point. Figure 3 shows the flow chart of modified Perturb and Observe (P&O) algorithm.

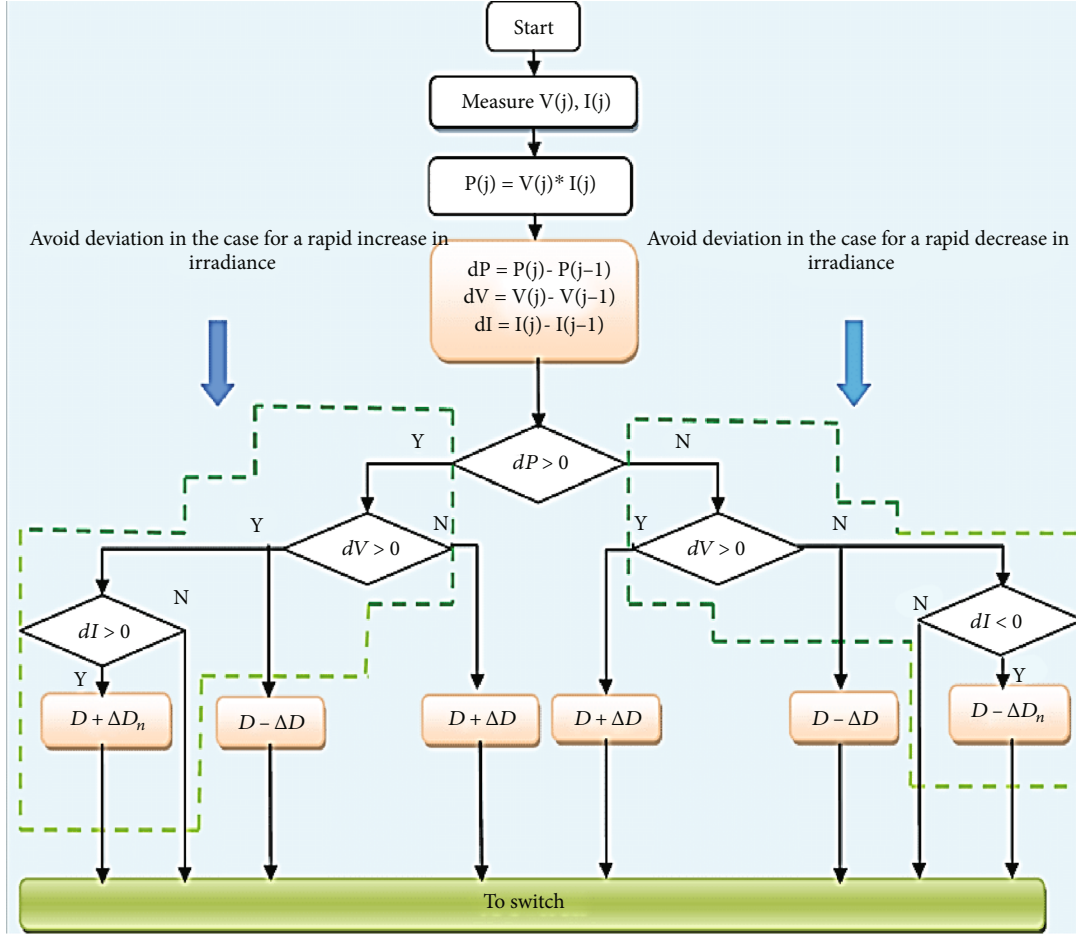


FIGURE 3: Flow chart of modified Perturb and Observe algorithm.

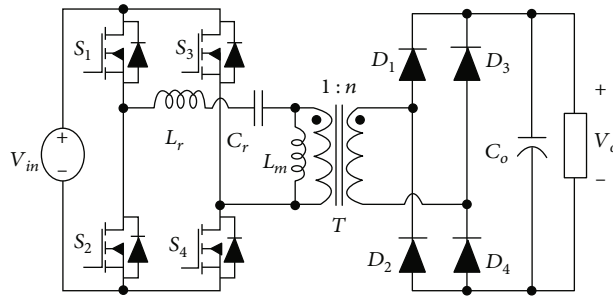


FIGURE 4: Circuit diagram of LLC Resonant converter.

The traditional P&O maximum power point tracking is based on the measurement of dP and dV while considering the PV module's P-V properties. As previously stated, conventional P&O suffer from deviation when irradiation changes due to confusion, which can be removed by analyzing another parameter dI (change in current) [1]

The conventional P&O method is incapable of meeting both the performance objectives of fast dynamic reaction and acceptable accuracy in the steady state. This is due to the fact that if the step-size is large enough for a fast-dynamic reaction, the oscillation around the maximum

TABLE 1: Design parameters of resonant voltage multiplier rectifier circuit.

Input values	50V-70V
Output values	415 V/425 W
$T_1 - T_6$	MOSFETs
Resonant inductor L_r	56.5 μ H
Resonant capacitor C_r	22.12 nF
Magnetizing inductance L_m	45.25 μ H
Turns ratio n	5 : 1
$D_1 - D_4$	Schottky diodes

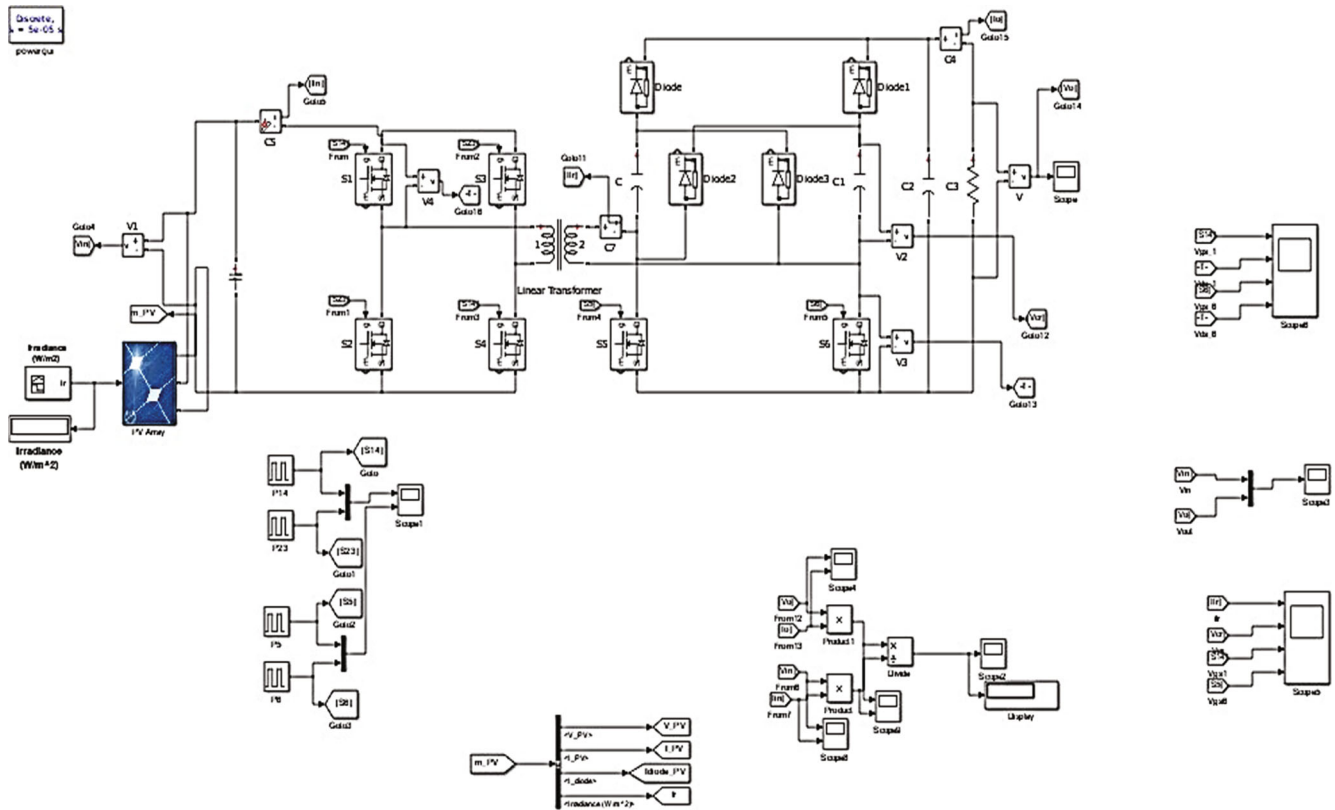


FIGURE 5: Simulation circuit diagram of modified resonant voltage multiplier rectifier topology.

power operating point will grow during the steady state, resulting in decreased power generation. The goal of the new strategy is to find an effective way to improve both dynamics and steady-state performance. [4]

Because the peak voltage on the two diodes is roughly 413 V, a 415 V rated diode can be used for D1 and D4, whereas a 610 V rated diode can be used for D2 and D4 because the voltage stress on the two diodes is equivalent to the output voltage of 415 V.

4. Design of Controller

This converter has two operating modes that must be controlled. A two-carrier modulation approach can be used to accomplish this. Figure 4 depicts the control block diagram as well as the modulation principle. Only the output of the PI regulator, V_{ctrl} , determines the phase-shift angles. Two carrier signals make up the phase-shift modulator. V_{n1} offsets the boost mode carrier. The modulator's output, d_s , is utilized to phase-shift modulate the secondary-side switches when V_{ctrl} is greater than V_{n1} . [9]

Because of the same characteristics, the traditional full-bridge LLC resonant converter depicted in Figure 4 was chosen for performance comparison.

Only the conduction losses are examined because both the LLC converter and the existing converter can be implemented with soft-switching devices. The magnetizing inductance, L_m , of the LLC resonant converter must be lowered to meet the required voltage conversion ratio since the circulat-

ing current introduced by the L_m is significantly larger than the suggested converter. The primary-side switches, transformer winding, resonant inductor, and resonant capacitor have larger current stresses and conduction losses than the proposed converter since the resonant tank is located on the primary side [2–5].

The LLC resonant converter's rectifier diodes have lower conduction losses than the proposed converter because the planned RVMR has two switches in addition to four diodes, whereas the LLC resonant converter only has four. The secondary-side current is substantially lower due to the high output voltage, and the voltage stresses of the two higher diodes, D1 and D4, as well as switches S5 and S6 in the existing converter, are lower than the rectifying diodes in the LLC resonant converter. To reduce power losses, low voltage diodes and switches with reduced conduction losses and higher switching performance can be employed.

A model with an isolated DC-DC conversion was created to validate the performance of the suggested converter, and a secondary control stage with a single source was designed.

A simulation model with a functional prototype was created to validate the functionality of the suggested converter, and the results are reported in Table 1. The converter's key functional processes are examined under various operating situations.

5. Simulation Results and Discussion

Figure 5 depicts the simulation diagram for the redesigned resonant voltage multiplier rectifier topology. Figure 6

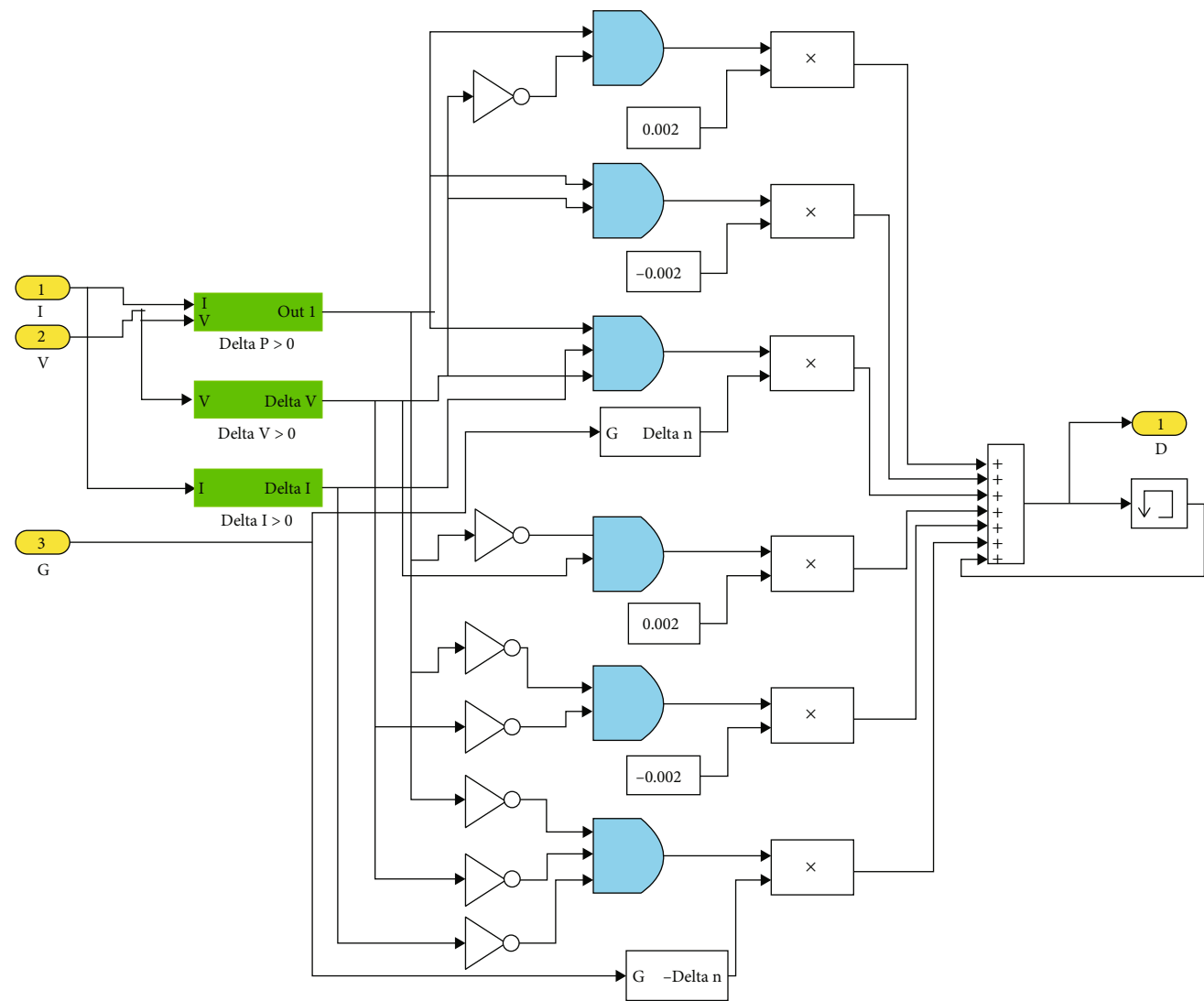


FIGURE 6: Simulation circuit diagram of modified Perturb and Observe algorithm.

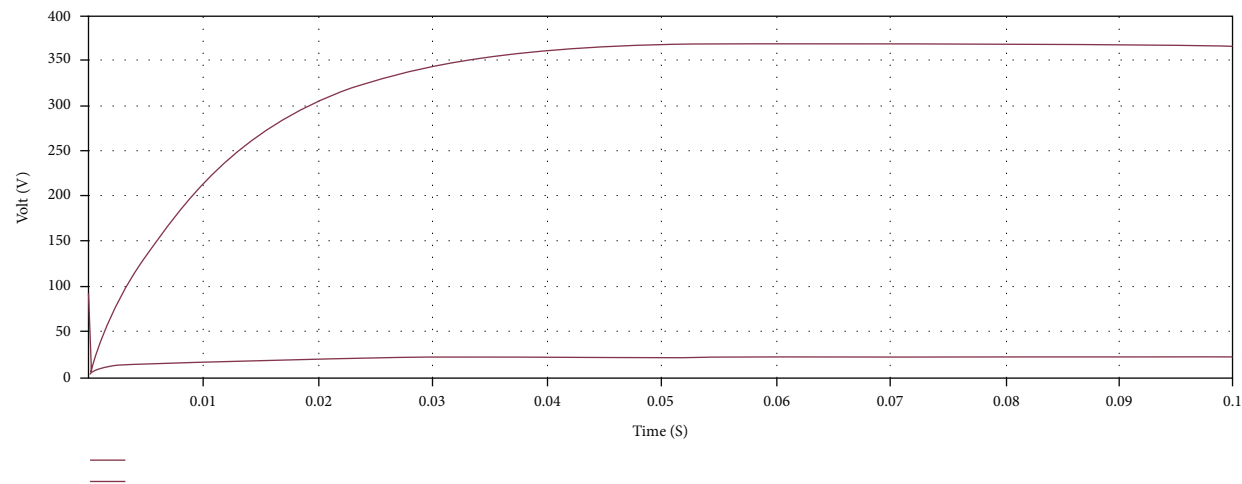


FIGURE 7: Output voltage waveform of boost mode.

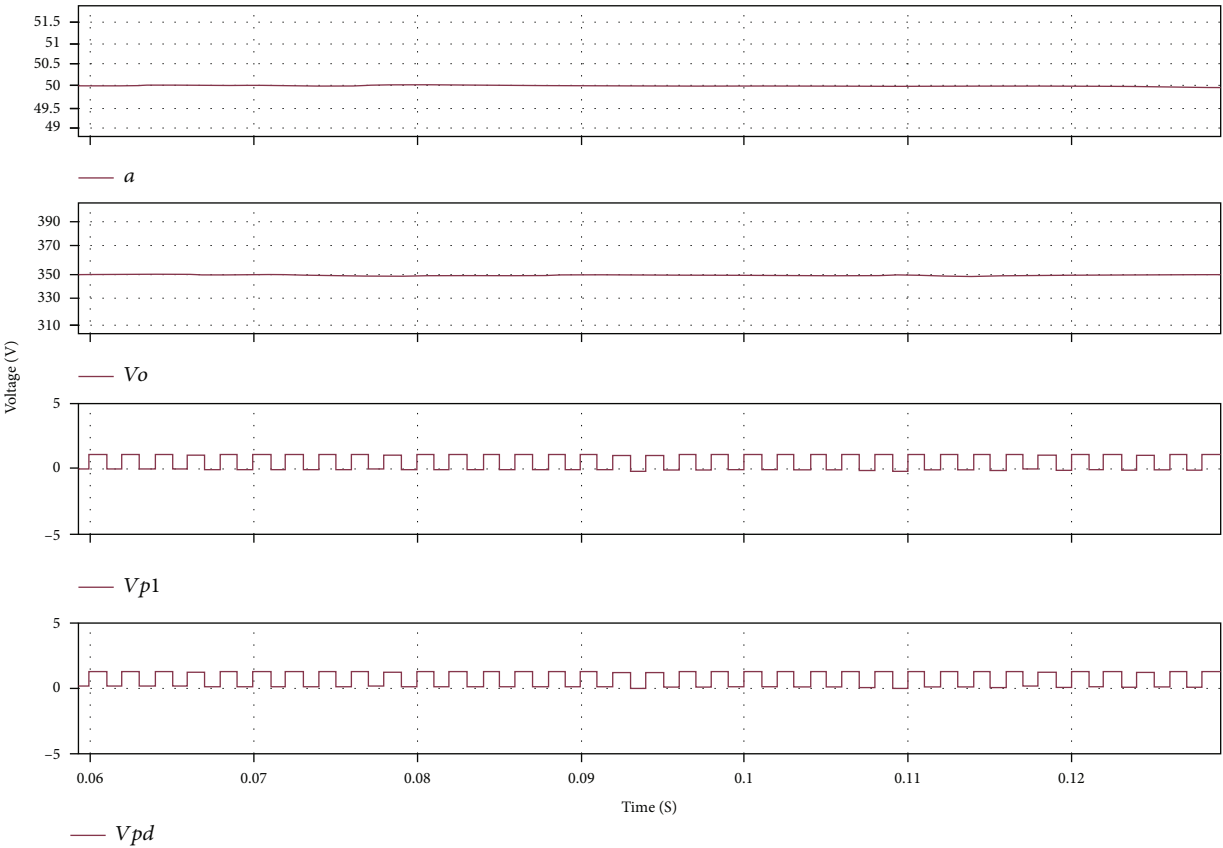


FIGURE 8: Output waveform of boost mode.

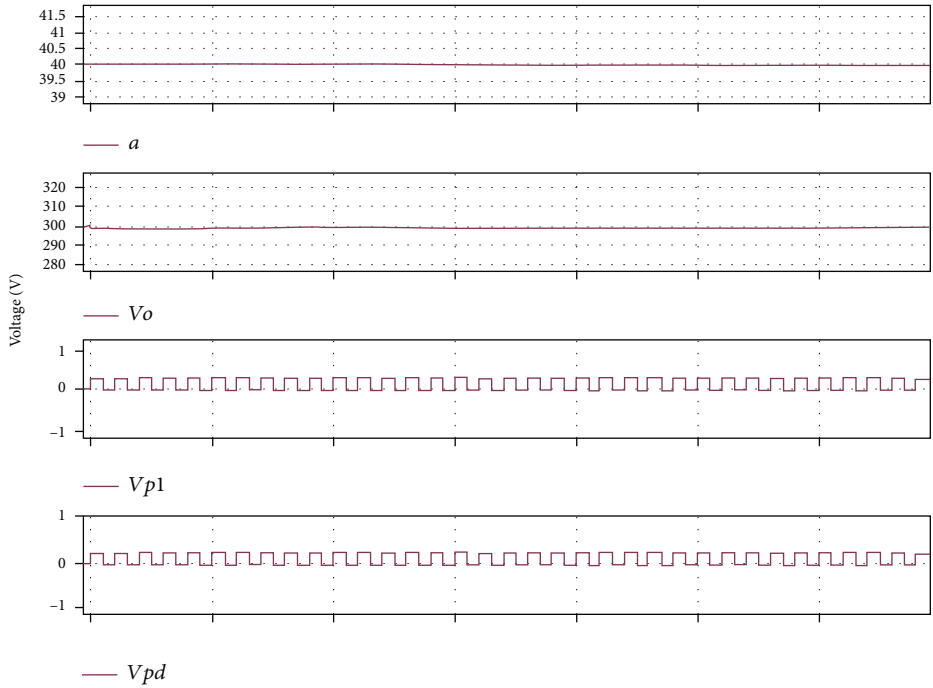


FIGURE 9: Output waveform of resonant switching state.

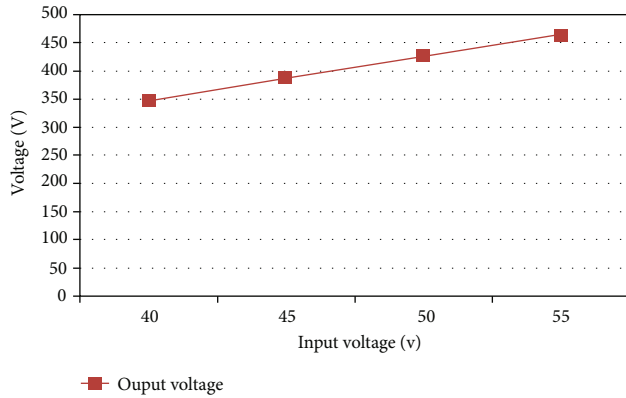


FIGURE 10: Input voltage vs. output voltage.

depicts the simulation circuit diagram of modified Perturb and Observe maximum power point algorithm.

Figure 7 depicts the converter's input and output voltages, as well as its PWM driving schemes. With $V_{in} = 55$ V and $V_{out} = 381$ V, it provides boost operation. The principal side switches S1 and S4 have a duty of 55%, whilst S2 and S3 have a phase-shift control of 1 s and a duty of 35%. The duty rating of the secondary-side switches is 47 percent.

Figure 8 shows the steady-state waveforms of the resonant inductor, resonant capacitor, and S1 and S6 driving voltages in boost mode.

Figure 9 shows the steady-state waveforms of the resonant inductor, resonant capacitor, and S1 and S6 driving voltages under half and full load in boost mode with 41 V input voltage.

Figure 10 shows the output voltage and input voltage for the same duty ratio control. The voltage increase on the input side is mirrored on the output, which tends to rise. Therefore, secondary-side voltage control can be used to maintain a constant voltage.

Figure 11 shows the efficiency curves versus input voltage under various output loads, demonstrating that high efficiency of more than 97 percent can be achieved over a wide voltage and load range. Peak efficiency is reached with a normalized voltage gain of $G = 1.1$ at 51 V input voltage.

When the voltage gain G is less than 1.1, the efficiency drops, comparable to a standard Buck-Boost converter. Even at a 15.1% output load, the converter achieves a high efficiency of 97 percent, demonstrating the converter's light-load efficiency.

The variation of power with a step change has been illustrated in Figure 12 to demonstrate the usefulness of the suggested method. The suggested technique has a faster tracking speed than typical trackers, settling at 0.22 s, and the tracker settles considerably faster under the step change by managing the efficiency around the maximum point.

Figure 13 depicts the change in solar irradiance and the step change efficiency pattern, which is settled around 0.156 s, and the efficiency is settled around 0.11 s without greater levels of oscillations when the irradiance changes.

Figure 14 displays the modified P&O MPPT, which shows that the converter is operated with a minimum settling time and a 95 percent efficiency.

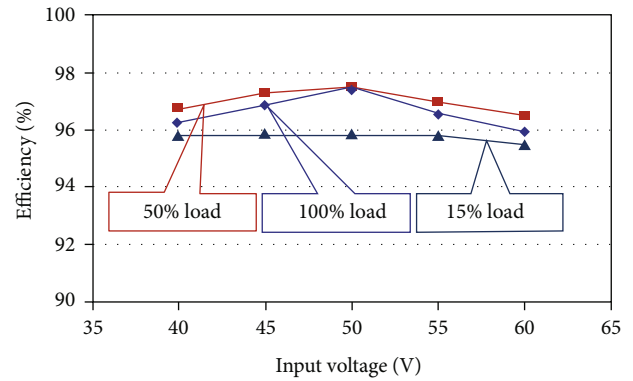


FIGURE 11: Input voltage vs. efficiency.

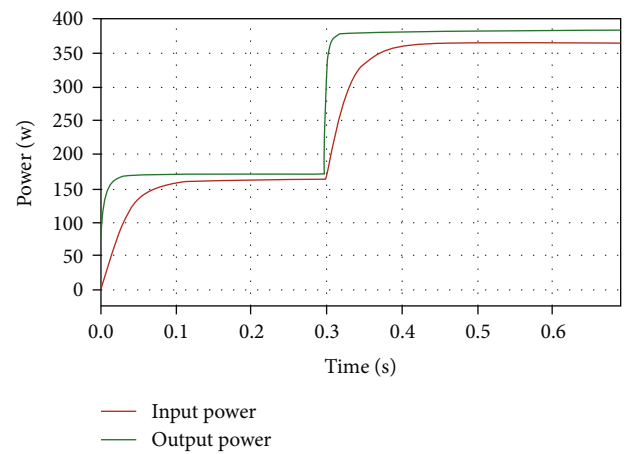


FIGURE 12: MPPT tracking with step variations of Input and output power.

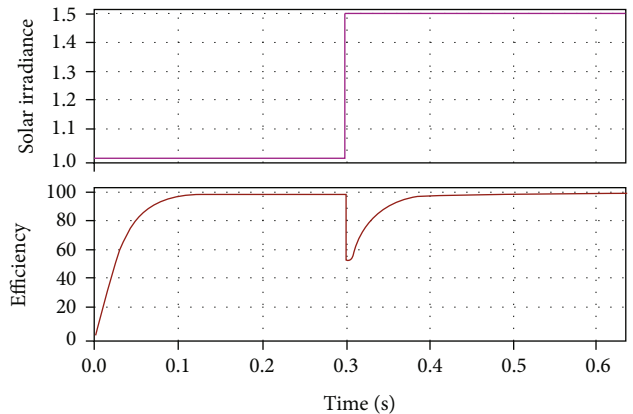


FIGURE 13: Step change variations of solar irradiance vs. efficiency.

The RVMR output voltage is shown in Figures 15(a)–15(e) for various input voltages. Table 2 shows the output voltage variation as a function of input voltage.

Figure 16 depicts the relationship between RVMR output voltage and input voltage. The input voltage vs. gain relationship is shown in Figure 17.

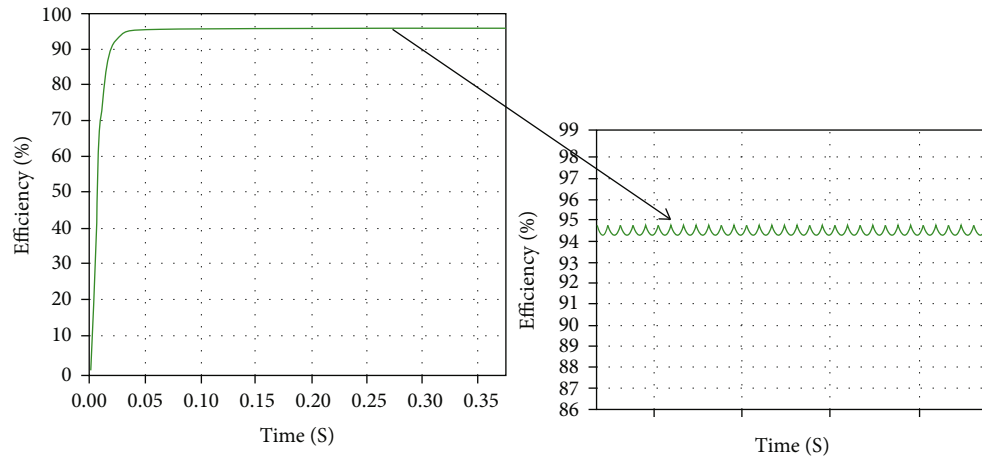


FIGURE 14: Output waveform of modified P&O under constant irradiance.

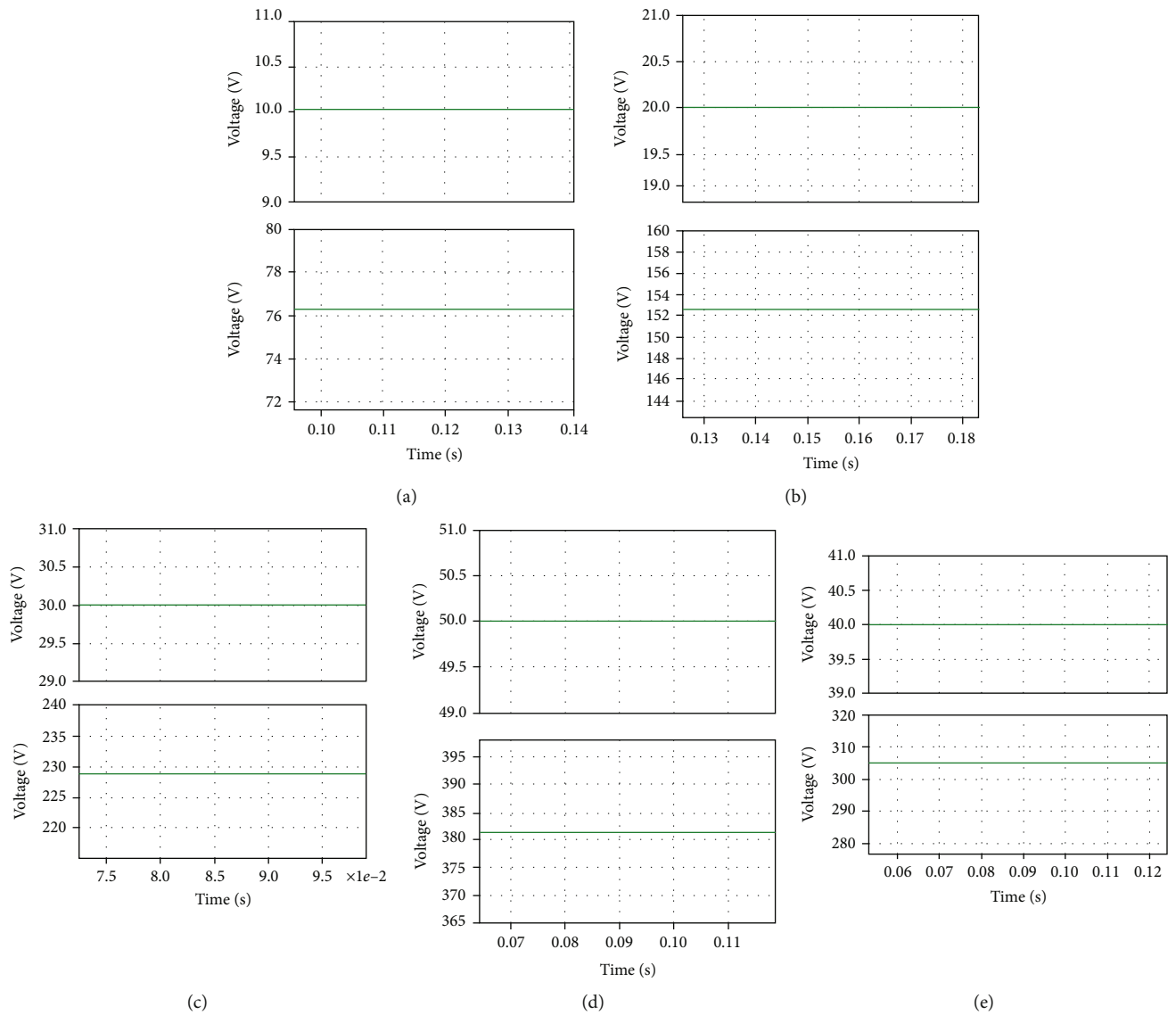


FIGURE 15: Output waveforms of resonant voltage multiplier rectifier output voltage. (a) Input voltage is 10 V, (b) input voltage is 20 V, (c) input voltage is 30 V, (d) input voltage is 40 V, and (e) input voltage is 50 V.

TABLE 2: Comparison of input voltage with boosted output voltage.

Input voltage (V_{in})	Boost voltage (V_{boost})
10	77
20	154
30	231
40	309
50	388

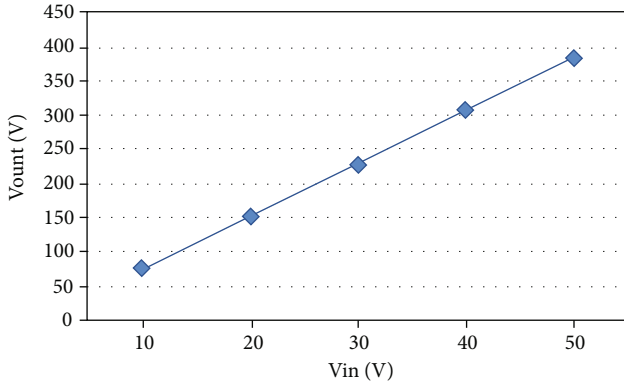


FIGURE 16: Comparisons of input and output voltage.

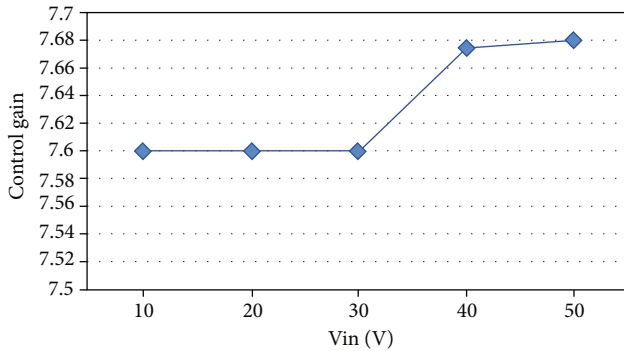


FIGURE 17: Comparisons of input voltage and control gain.

6. Conclusion

This paper focuses on a modified RVMR-based photovoltaic source. It was possible to integrate a modified RVMR with a photovoltaic grid-connected system. The simulation findings reveal that the redesigned RVMR's operating characteristics result in a high DC-DC voltage gain and higher efficiency. Unlike traditional DC-DC boost converters, the proposed RVMR combines the functions of a switching capacitor and a voltage multiplier, resulting in a high voltage gain for a wide range of input voltages. As a result, this design is preferable in terms of fast dynamic response and high voltage gain for a cascaded PV module for real-time applications. These advancements in DC-DC boost converter technology will surely allow for more powerful and innovative power converter solutions in the next generation of power conversion systems. A new RVMR-based converter has been developed. The maximum power from PV is

extracted using a P&O-based MPPT approach. The upgraded RVMR outperforms the QZSI, and the voltage gain is significantly higher when compared to other converters. The RVMR, on the other hand, necessitates a lot of space due to its bulkiness. A hybrid renewable energy system can benefit from a bidirectional battery charger. The presented approach can incorporate renewable energy sources such as fuel cells and biomass. FPGAs can be used to implement the control digitally. Total harmonic distortion (THD) and power quality analysis can also be included.

Data Availability

The data used to support the findings of this study are included within the article.

Disclosure

It was performed as a part of the Employment of Authors.

Conflicts of Interest

The authors declare that they have no conflicts of interest.

References

- [1] L. Gelažanskas, A. Baranauskas, K. A. A. Gamage, and M. Azubalis, "Hybrid wind power balance control strategy using thermal power, hydro power and flow batteries," *Journal of Electrical Power and Energy Systems*, vol. 74, pp. 310–321, 2016.
- [2] R. Teodorescu, M. Liserre, and P. Rodriguez, *Grid Converters for Photovoltaic and Wind Power Systems*, A John Wiley and Sons, Ltd, 2016.
- [3] R. Ramkumar, M. V. Kumar, and D. Sivamani, "Fuzzy logic based soft switched active clamped boost converter charging strategy for electric vehicles," in *2020 4th International Conference on Electronics, Communication and Aerospace Technology (ICECA)*, pp. 1334–1339, Coimbatore, India, 2020.
- [4] R. Ravindran, C. R. Sathiasamuel, P. Ramasamy, and K. Balasubramanian, "MSVM-based hybrid energy-fed quasi-Z-source cascaded H-bridge inverter for grid-connected system," *International Transactions on Electrical Energy Systems*, vol. 31, no. 12, article e13139, 2021.
- [5] R. S. Preethishri and K. Selvi, "The Photovoltaic module fed Push Pull converter with MPPT controller for Solar energy applications," in *2016 IEEE 1st International Conference on Power Electronics, Intelligent Control and Energy Systems (ICPEICES)*, pp. 1–4, Delhi, India, 2016.
- [6] S.-J. Chen, S.-P. Yang, and C.-M. Huang, "Interleaved high step-up DC-DC converter with parallel-input series-output configuration and voltage multiplier module," in *IEEE International Conference on Industrial Technology (ICIT)*, vol. 8, pp. 119–124, Toronto, ON, Canada, 2015.
- [7] A. V. Sieber, H. Haimovich, and M. E. Romero, "Control-oriented modelling and adaptive control of a single-phase quasi-Z-source inverter," in *IECON 2013 - 39th Annual Conference of the IEEE Industrial Electronics Society*, pp. 572–577, Vienna, Austria, 2013.
- [8] M. Forouzesh, Y. Shen, K. Yari, and Y. Siwakoti, "A new soft-switched high step-up DC-DC converter with dual coupled

- inductors,” in *2017 IEEE 12th International Conference on Power Electronics and Drive Systems (PEDS)*, pp. 863–868, Honolulu, HI, USA, 2017.
- [9] M. Forouzesh, Y. P. Siwakoti, S. A. Gorji, F. Blaabjerg, and B. Lehman, “Step-up DC–DC converters: a comprehensive review of voltage-boosting techniques, topologies and applications,” *IEEE Transactions on Power Electronics*, vol. 32, no. 12, pp. 9143–9178, 2017.
- [10] M. K. Sahu and N. Kumar, “Fuel cell system using high step-up converter with voltage multiplier module,” *International Journal of Software and Hardware Research in Engineering*, vol. 3, pp. 54–65, 2015.
- [11] S. Sun, M. Dong, and B. Liang, “Real-time power balancing in electric grids with distributed storage,” *IEEE Journal on Selected Topics in Signal Processing*, vol. 8, no. 6, pp. 1167–1181, 2014.
- [12] B. Ge, H. Abu-Rub, F. Z. Peng et al., “An energy-stored quasi-Z source inverter for application to photovoltaic power system,” *IEEE Transactions on Industrial Electronics*, vol. 60, no. 10, pp. 4468–4481, 2013.
- [13] M. Muthukumaran, S. Sankarkumar, and M. Sureshkumar, “A modified SEPIC converter with high static gain for renewable applications,” *International Journal on Advanced Electrical and Computer Engineering*, vol. 2, pp. 76–85, 2015.
- [14] H. M. El-Helw, A. Magdy, and M. I. Marei, “A hybrid maximum power point tracking technique for partially shaded photovoltaic arrays,” *IEEE Transactions and Content Mining are Permitted for Academic Research*, vol. 5, pp. 11900–11908, 2017.
- [15] P. Kinjal, K. B. Shah, and G. R. Patel, “Comparative analysis of P&O and INC MPPT algorithm for PV system,” in *2015 International Conference on Electrical, Electronics, Signals, Communication and Optimization (EESCO)*, Visakhapatnam, India, 2015.
- [16] A. A. Kulaksiz, “ANFIS-based estimation of PV module equivalent parameters: application to a stand-alone PV system with MPPT controller,” *Turkish Journal of Electrical Engineering and Computer Sciences*, vol. 21, no. 2, pp. 2127–2140, 2013.
- [17] U. Nandhalaalaa, S. Ramkumar, and M. Muruganandam, “High static gain for solar application using modified SEPIC converter,” *International Journal of Innovative Research in Science, Engineering and Technology*, vol. 4, pp. 34–41, 2015.
- [18] N. Azura, S. Iqbal, and S. Taib, “LLC resonant DC–DC converter for high voltage applications,” in *2014 IEEE Conference on Energy Conversion (CENCON)*, vol. 6, pp. 90–95, Johor Bahru, Malaysia, 2014.
- [19] S. Jain and V. Agarwal, “A single-stage grid connected inverter topology for solar PV systems with maximum power point tracking,” *IEEE Transactions on Power Electronics*, vol. 22, no. 5, pp. 1928–1940, 2007.